Front. Earth Sci. 2025, 19(1): 25−40
https://doi.org/10.1007/s11707-021-0949-y

RESEARCH ARTICLE

# Monitoring the trophic state of shallow urban lakes using Landsat 8/OLI data: a case study of lakes in Hanoi (Vietnam)

**Pham Quang VINH[1], Nguyen Thi Thu HA (✉)[2], Nguyen Thien Phuong THAO[2], Nguyen Thuy LINH[2,3], La Thi OANH[4], Luong Thi PHUONG[3,5], Nguyen Thi Thu HUYEN[1]**

1 Institute of Geography, Vietnam Academy of Science and Technology, Hanoi 10000, Vietnam
2 Faculty of Geology, VNU University of Science, Vietnam National University, Hanoi 10000, Vietnam
3 Faculty of Geography, VNU University of Science, Vietnam National University, Hanoi 10000, Vietnam
4 Department of Geomatics, Cheng Kung University, Tainan 70101, China
5 The Alliance of Biodiversity International and CIAT, Hanoi 10000, Vietnam



**Abstract** Lakes in the Hanoi urban areas are highly vulnerable to serious eutrophication and algae bloom due to anthropogenic pollution and climate change. This study aims at monitoring the trophic state of lakes in Hanoi by developing an empirical model for directly estimating the trophic state index (TSI) from Landsat 8 (L8) level 2 data, which has been atmospheric corrected by the Land Surface Reflectance Code (LaSRC) algorithm and provided freely by the US Geological Survey (USGS). Regression analysis of a 138-point data set of *in situ* TSI measured in 13 lakes in Hanoi on seven dates in the 2015–2020 time period with the simultaneously acquired L8 reflectance data set showed a significant correlation between TSI and L8 spectral ratio of the near-infrared band (band 5) versus the green band (band 3) by a logarithmic equation (the coefficient of determination, $R^2$ = 0.65). Validation results demonstrated that the model was appropriate for estimating TSI in highly trophic waters (the root-mean-square error, RMSE = 6.6). The model then was applied to six selected L8 images to observe an increasing trend in TSI of 25 lakes in the Hanoi urban area during the 2015–2020 time period. The L8-LaSRC performed better than the Landsat 8 Provisional Aquatic Reflectance Product in providing data for monitoring shallow urban lakes. Our proposed model can be applied to monitor the TSI of worldwide lakes with similar features as lakes in the Hanoi urban areas.

**Keywords** TSI, urban lakes, eutrophication, LaSRC, L8PAR

Received February 21, 2021; accepted October 22, 2021

E-mail: hantt_kdc@vnu.edu.vn

## 1 Introduction

Urban lakes are inland water bodies surrounded by an urban environment (Persson, 2012) and are often shallow, highly artificial, and even hypertrophic (Birch and McCaskie, 1999). Despite their small and shallow nature, urban lakes play a vital role in enhancing urban landscape and providing environmental and social-economic services, e.g., regulating storm water, providing places for recreation, supporting urban biodiversity, and providing livelihoods. The quality and quantity of water in urban lakes are strongly influenced by urbanization (Yang et al., 2007; Yang and Ke, 2015). In particular, urban lakes often receive a high nutrient and heavy metal load from runoff due to contributions from municipal wastewater discharges and sewage overflows. Consequently, urban lakes are especially susceptible to eutrophication, toxic pollution, and harmful algal blooms. Hence, monitoring urban lake water quality, particularly monitoring and assessing the lake's trophic state, is indispensable in urban environmental management to understand the dynamics of the environmental quality and possible impacts of urbanization on wildlife.

A lake's trophic state is a concept that aims to quantify the productivity of a waterbody and evaluate its usability for fishing or swimming (Carlson and Simpson, 1996). Hence, determining the lake trophic state is an essential aspect of urban lake management because it provides information about lake ecosystem services (e.g., clean water, recreational opportunities, and aesthetics) and risks (e.g., cyanobacteria blooms, high turbidity). The lake trophic state has been determined using various indices, the most well-known among them being the trophic state index (TSI), developed by Carlson (1977). Carlson's TSI is calculated from three variables, i.e., chlorophyll a concentration (Chla), total phosphorus concentration (TP), and the Secchi depth (SD). The TSI value ranges from zero to 100 and can assign a trophic state "grade" to a lake. Accordingly, lakes are commonly classified according to their trophic state, based on trophic state categories, into four levels: oligotrophic, mesotrophic, eutrophic, and hypertrophic (Carlson and Simpson, 1996).

The traditional method to determine the lake trophic state is a lake survey where TSI can be calculated at each survey point using *in situ* data of Chla, TP, and SD. This is a costly and time-consuming method for monitoring the trophic state of many lakes over a large region. Remote sensing has been successfully used over the past 40 years to estimate lake water quality worldwide, particularly in monitoring trophic variables such as SD and Chla (Chang et al., 2015; Gholizadeh et al., 2016). Using satellite imagery to assess and monitor the lake trophic state is a possible and promising application (Fuller and Jodoin, 2016; Membrillo-Abad et al., 2016) that helps overcome the challenges of the traditional lake survey method. Among numerous optical satellite data, Landsat 8 (L8) data have been recognized as a tool with high potential for retrieving water quality parameters such as Chla (Boucher et al., 2018; Buma and Lee, 2020) and SD (Olmanson et al., 2016; Ren et al., 2018) in inland lake waters, even for small and shallow lakes in urban areas (Ha et al., 2017a; Zhu et al., 2020). The temporal coverage and spatial resolution of L8 and its easy accessibility are primary reasons to select this sensor for monitoring the trophic state of urban lakes. Moreover, L8 bands are located in all of the main color segments of the visual domain and are narrower than previous Landsat imagery, providing more opportunity for the establishment of empirical models for water retrievals (Chen et al., 2020). Several studies have employed L8 data for estimating TSI of lakes (Shi et al., 2019; Zhou et al., 2019; Chen et al., 2020; Kumar Jally et al., 2020), proving L8 data as a promising tool to assess and monitor the lake trophic level.

Up to present, there are two approaches to estimate TSI directly from remote sensing data, i.e., using a semi-analytical algorithm (Shi et al., 2019) and using a machine learning model (Zhou et al., 2019). The semi-analytical algorithm analyzed the relationships of *in situ* TSI with water's inherent optical properties (IOP), such as the total absorption coefficient, $a(\lambda)$, and the total backscattering coefficient, $b_{bp}(\lambda)$, derived from $R_{rs}(\lambda)$ (Shi et al., 2019). The semi-analytical algorithm does not need recalibrating data and can be applied to different water types, but its performance relies on the accurate spectral models for estimating IOP components for each water constituent (Chen et al., 2018). The uncertainty of the semi-analytical algorithm has been reported in previous studies (Jiang et al., 2019; Liu et al., 2020) on the errors in deriving the diffuse attenuation of down-welling irradiance ($K_d$, $m^{-1}$), $a(\lambda)$, from $R_{rs}(\lambda)$. Moreover, the use of the semi-analytical algorithm is time-consuming and contains a complicated procedure for estimating Chla (Rotta et al., 2021) and SDD (Jiang et al., 2019; Liu et al., 2020) before calculating TSI, which is limited in processing a large data set. Therefore, the semi-analytical algorithm is inappropriate for water quality monitoring at the local level which requires a simple but effective technique. The machine learning model, the radial basis function (RBF) neural network, was used to estimate TSI directly from L8 data by Zhou et al. (2019) based on the constructions of the input layer parameters from band combinations with water information and the output layer of the TSI. The limitation in the number of training data (33 points) and testing data (10 points) challenged the model's applicability in a broad region with various water trophic levels and seasonal fluctuation of TSI. The band-ratio method, with the advantage of reducing the atmospheric and topological effects, was also shown in the study of Zhou et al. (2019).

An empirical model for a direct estimation of TSI from L8 data has been missing in previous studies. The empirical model is often developed by direct regression analysis between the remote sensing data, the remote sensing reflectance, and *in situ* TSI calculated by one or more indicators (Chla, SD, and TP) measured simultaneously. The empirical model requires a wide range of matching *in situ* measurements and is location/region-dependent (Lee et al., 2016). However, as Matthews (2011) stated, the empirical approach has a demonstrable high capability in water quality monitoring because of its simple yet robust procedures. In addition, the algorithm can be applied to diverse waters affected by similar weather and hydrological conditions if the empirical algorithm is developed based on a data set measured from broadly varied bio-geophysical and optical waters.

The primary challenge in using L8 data for monitoring the trophic state level of inland lakes is the atmospheric correction (AC) process because most water reflectance signals received by satellite sensors are affected by the atmosphere (Mouw et al., 2015). Many AC methods for L8 data have been developed (such as Dark Object Subtraction (DOS), QUick Atmospheric Correction (QUAC), Fast Line of Sight Atmospheric Analysis of Spectral Hypercubes (FLAASH), Atmospheric Correction for OLI 'Lite' (ACOLITE) ) and evaluated for the application in retrieving water quality parameters (Bernardo et al., 2017; Ha et al., 2017a; Pham et al., 2018). Among them, FLAASH has been proposed as the most accurate AC method for water retrievals in inland waters (Ha et al., 2017a; Pham et al., 2018). However, the procedure of FLAASH is complicated and time-consuming for the purpose of long-term monitoring that requires high quality in human resources and facilities. Since 2017, the US Geological Survey (USGS) has provided the atmospheric corrected L8 data (L8 level 2) to all users freely, from which L8 data are generated by using the algorithm called Land Surface Reflectance Code (LaSRC) (Vermote et al., 2016). The L8 LaSRC data have been evaluated as promising for water constituent retrievals in inland waters (Kuhn et al., 2018; Pham et al., 2018; Dave et al., 2019). On April 1st, 2020, the USGS/ESPA released the Landsat 8 Provisional Aquatic Reflectance Product (L8PAR) which provides water surface reflectance for water constituent retrievals. This product was preliminarily evaluated as inappropriate for retrievals in small and turbid inland waters because of providing negative values for almost all pixels of the water bodies (Ogashawara et al., 2020). Further validation is still needed to evaluate the performance of L8PAR data for water quality monitoring purposes.

Hanoi city, the capital of Vietnam, is sometimes called "the city of lakes" because, in only six core districts of the city (viz. Ba Dinh, Hoan Kiem, Dong Da, Hai Ba Trung, Cau Giay, and Tay Ho), there are 112 lakes and ponds (CECR, 2015). Lakes in the Hanoi urban area play a vital role in regulating stormwater, reducing flooding and inundation, providing spots for sightseeing, recreation, entertainment, and festivals. Despite their important role, lakes in the Hanoi urban areas face many serious problems such as pollution due to domestic garbage and untreated wastewater, water surface reduction due to illegal encroachment of the lake corridor, and levelling for construction land (CECR, 2010; Lap et al., 2013). Many preceding domestic studies also confirmed that these lakes are classified as highly eutrophic to hypertrophic (Ha et al., 2016; Nguyen et al., 2016; Han et al., 2017; Hoang et al., 2017; Thủy et al., 2017). Lakes in Hanoi are representatives of urban lakes worldwide, which are always at highly trophic levels and required frequent monitoring.

This study aims to develop an empirical model to estimate the TSI in small, shallow, and highly trophic urban lakes from L8 LaSRC data. In this study, a 138-point *in situ* TSI, which was calculated from *in situ* measured Chla and SD over 13 lakes in Hanoi, was cross-regressed with the L8 LaSRC-derived water reflectances acquired at the same time with the field measurements. In this study, both L8-LaSRC and L8PAR data were also evaluated using *in situ* water reflectance measured in West Lake on August 13th, 2019. The proposed models were then applied to multiple-date L8 scenes to identify the changes of TSI of lakes in the Hanoi urban area in a 5-year period and TSI dynamics of West Lake during the summer of 2015–2020.

## 2 Materials and methods

### 2.1 Studied lakes

Figure 1 illustrates the locations of studied lakes in Hanoi city (Vietnam). Among 13 surveyed lakes, 12 lakes (i.e., Ho Tay Lake, Nghia Tan Lake, Thu Le Lake, Giang Vo Lake, Dong Da Lake, Nam Dong Lake, Ba Mau Lake, Bay Mau Lake, Thien Quang Lake, Linh Dam Lake, Hoan Kiem Lake, and Van Quan Lake) are located in the Hanoi urban areas, and they all are featured as small (the water surface area ranges from area 0.4 to 400 ha), shallow (the average depth is 2–3 m), and of high turbidity (the average SD < 0.5 m) (CECR, 2015). Algae blooms occurred frequently in several lakes such as Van Quan Lake and Hoan Kiem Lake, bringing floating green scum and foul smells (Vietnamnet.vn, 2016; Vnexpress.net, 2018; Vietnamnews.vn, 2016, 2018), indicating a very high trophic level of these two lakes, which can be recognized as the top bound of TSI values used in this study. In contrast, Dong Mo Lake is a reservoir located in the city belt with a total water surface area of 650 ha and an average depth of 5 to 10 m (Fig. 1) and was selected to provide the low bound of TSI values for this study

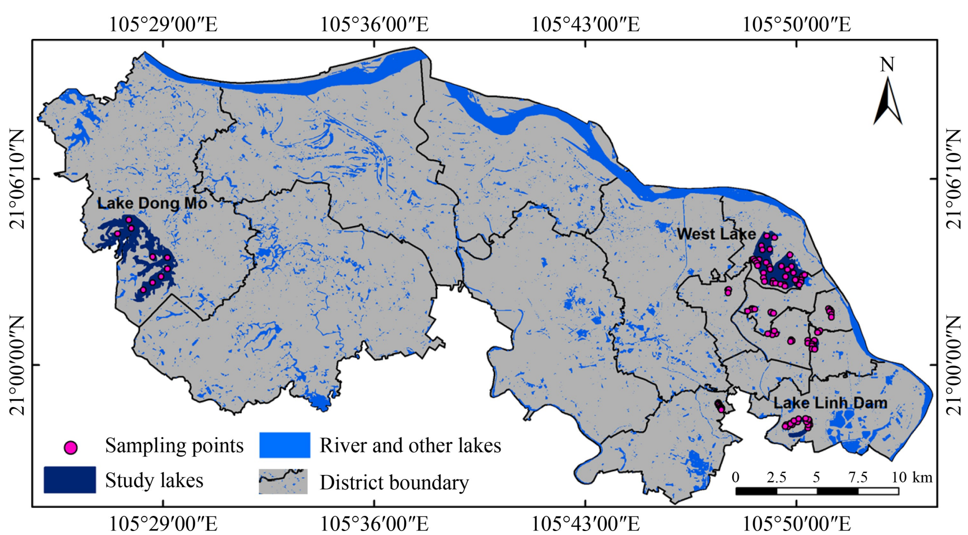


**Fig. 1** Distribution of 13 studied lakes (dark blue areas) and locations of measured points in Hanoi.

because the lake trophic level is lower than lakes in the Hanoi urban area.

### 2.2 Field measurement and sampling

*In situ* data were collected at 138 points over 13 studied lakes during seven field campaigns in 2016, 2017, and 2019. At each point, the water sample was collected at a depth of 30 cm using a Van Dorn water sampler and kept in 1-L cleaned darkly colored bottles. In the laboratory, the water samples were analyzed to determine Chla, the photosynthetic pigment concentration that indicates the amount of algae living in the water, based on the standard spectrophotometrically method (10200-H) of the American Public Health Association (APHA, 1998), which used a DR 5000 UV-VIS Laboratory Spectrophotometer (Hach, Colorado, U.S) with a 1 nm spectral bandwidth resolution. SD was measured in the field using a standard 20 cm diameter plastic Secchi disk (model 3-58-B10, Wildco, Florida, U.S). To avoid direct sunlight reflections from the water, SD was measured on the ship's shaded side and determined by the arithmetic average of a total of three readings.

Above-water surface reflectance measurements were also taken using the GER1500 spectroradiometer (Spectra Vista Corporation, New York, US) by the above-water reflectance measurement method (Mueller et al., 2003). Water reflectance, $\rho_\omega(\lambda)$ at each measured point was calculated using the following equation:

$$\rho_\omega(\lambda) = R_\mathrm{p} \cdot \left(\frac{L_\mathrm{w}(\lambda) - r \cdot L_\mathrm{sky}(\lambda)}{\pi \cdot L_\mathrm{p}(\lambda)}\right), \tag{1}$$

where $R_\mathrm{p}$ is the reflectance of the reference panel; $L_\mathrm{w}(\lambda)$ is the radiance of water-viewing; $L_\mathrm{sky}(\lambda)$ is the radiance of sky measured sequentially at 40–45 degrees from nadir and zenith, respectively, and 135 degrees from the Sun in azimuth (Mobley, 1999); $r$ is the air−water interface reflectance with a value of 0.028; and $L_\mathrm{p}(\lambda)$ is the radiance of the reference panel. In this study, the above water surface reflectance data aids in understanding the optical features of studied lakes and evaluating atmospheric corrected products' performance.

### 2.3 TSI determination

TSI based on Chla ($\mathrm{TSI_{Chla}}$) and TSI based on SD, ($\mathrm{TSI_{SD}}$) were determined from *in situ* Chla and SD according to equations developed by Carlson (1977), which were simplified by Carlson and Simpson (1996) as the following:

$$\mathrm{TSI_{Chla}} = 9.81 \cdot \ln(\mathrm{Chla}) + 30.6, \tag{2}$$

where the unit of Chla is μg/L and $\mathrm{TSI_{Chla}}$ is a non-dimensional number, and

$$\mathrm{TSI_{SD}} = 60 - 14.4 \cdot \ln(\mathrm{SD}), \tag{3}$$

where the unit of SD is in meters and $\mathrm{TSI_{SD}}$ is a non-dimensional number.

The *in situ* TSI was calculated from $\mathrm{TSI_{Chla}}$ and $\mathrm{TSI_{SD}}$ by the equation

$$\mathrm{TSI} = \frac{\mathrm{TSI_{Chla}} + \mathrm{TSI_{SD}}}{2}, \tag{4}$$

where all TSI, $\mathrm{TSI_{Chla}}$ and $\mathrm{TSI_{SD}}$ are non-dimensional numbers.

TP was not used to calculate TSI in this study because $\mathrm{TSI_{TP}}$ is often related to $\mathrm{TSI_{Chla}}$ and $\mathrm{TSI_{SD}}$ by linear regression models and has a nearly similar value to these index variables. In other words, TSI, calculated from $\mathrm{TSI_{Chla}}$ and $\mathrm{TSI_{SD}}$, can classify the lake trophic level (Carlson and Simpson, 1996). In addition, TP is an inactive optical parameter (Gholizadeh et al., 2016), and $\mathrm{TSI_{TP}}$, therefore, cannot be estimated directly from L8 data. Using the averaging TSI values of $\mathrm{TSI_{Chla}}$ and $\mathrm{TSI_{SD}}$ provides a better comparison of the estimated TSI in this study to the estimates of other studies using L8 data.

### 2.4 Landsat 8

Seven L8 scenes of path 127 and row 45, acquired on the same dates as the water measurements, were used to build the TSI estimation model, and their information is listed in Table 1. Additionally, an L8 scene which acquired on July 1st, 2015, over Hanoi city was also employed to validate the TSI estimation model because its acquiring time was closest to the time of water measurement by the Center for Environment and Community Research (CECR) (CECR, 2015), July 7th 2015. All eight of these L8 scenes were ordered and downloaded from the USGS Earth Explorer website via the on-demand interface. These L8 scenes all were computed for bottom-of-atmosphere (BOA) reflectance (surface reflectance) by the Land Surface Reflectance Code (LaSRC) algorithm (Vermote et al., 2016), which used auxiliary input data (i.e., water vapor, ozone, and elevation) from Moderate Resolution Imaging Spectroradiometer (MODIS) and the Earth Topography Five Minute Grid (ETOP05) to generate surface reflectance from Top of Atmosphere (TOA) Reflectance (USGS, 2020a). The LaSRC-based L8 surface reflectance data (hereafter referenced as L8-LaSRC) were designed for land applications but have also been exploited successfully for water constituent retrievals in riverine waters (Bernardo et al., 2017; Pham et al., 2018; Allam et al., 2020). Therefore, a further evaluation of the L8-LaSRC performance for water constituent retrieval in other inland waters, particularly lake water, is still needed.

In this study, we also evaluated the performance of L8PAR for retrieving remote sensing surface reflectance, $R_{rs}(\lambda)$ in small and shallow inland waters through the case of lakes in the Hanoi urban area. The L8 scene used for the evaluation was acquired on August 13th 2019 over Hanoi city and ordered via the USGS EROS ESPA

**Table 1** Information of L8 scenes used

| No. | Scene ID | Date | Product | Purpose |
|---|---|---|---|---|
| 1 | LC81270452015182LGN01 | July 1st 2015 | L8-LaSRC | Validation |
| 2 | LC81270452016153LGN01 | June 1st 2016 | L8-LaSRC | Model building |
| 3 | LC81270452016281LGN02 | October 7th 2016 | L8-LaSRC | Model building |
| 4 | LC81270452017091LGN00 | April 1st 2017 | L8-LaSRC | Model building |
| 5 | LC81270452017155LGN00 | June 4th 2017 | L8-LaSRC | Model building |
| 6 | LC81270452018158LGN00 | June 7th 2018 | L8-LaSRC | Mapping |
| 7 | LC81270452019177LGN00 | June 26th 2019 | L8-LaSRC | Mapping |
| 8 | LC81270452019225LGN00 | August 13th 2019 | L8-LaSRC and L8PAR | Model building/AC evaluation |
| 9 | LC81270452019337LGN00 | December 3rd 2019 | L8-LaSRC | Model building |
| 10 | LC81270452020180LGN00 | June 28th 2020 | L8-LaSRC | Mapping |

on-demand interface. The L8PAR generates $R_{rs}(\lambda)$ based on the Landsat Provisional Aquatic Reflectance algorithm (Mobley et al., 2016) operating in the Sea-viewing Wide Field-of-View Sensor (SeaWiFS) Data Analysis System (SeaDAS) package. The $R_{rs}(\lambda)$ was computed by converting the TOA reflectance into the water-leaving radiance, then normalizing the water-leaving radiance by down-welling the solar irradiance (USGS, 2020b). In both L8-LaSRC and L8PAR cases, water surface reflectance, $\rho_\omega(\lambda)$ is computed from a division of $R_{rs}(\lambda)$ by $\pi$ for the comparisons with *in situ* reflectance.

Finally, a density slicing integrated in ENVI 5.3 was applied to L8-LaSRC data to map the TSI distribution using various intervals to better visualize the spatial distribution of TSI and its change.

## 3 Results

### 3.1 Trophic state of lakes in Hanoi

The results from 138 points measured over 13 lakes in Hanoi on seven different dates, of which L8 acquired data are shown in Table 2, indicated a high trophic status of studied lakes. *In situ* Chla over 105 measured points ranged widely from 30.5 μg/L to 566.82 μg/L, averaged at 163.45 μg/L, suggesting that these lakes' water contained an abundance of phytoplankton. *In situ* SD measured at 93 points ranged from 0.05 m to 1.4 m with a mean value of 0.39 m. The highest SD value was recorded at Dong Mo Reservoir, where *in situ* Chla was missing. The highest SD value measured in lakes in the Hanoi urban area was 0.58 m (recorded at Lake Linh Dam on April 1st 2017). The lake waters in the Hanoi urban area can be classified as highly turbid waters with the main suspended particulates being phytoplankton which is evidenced by a strong correlation of SD and Chla (the Pearson correlation coefficient, $R = -0.77$).

*In situ* TSI values calculated from *in situ* Chla and SD by Eqs. (2), (3), and (4) ranged from 55 to 100, corresponding to the eutrophic level (50 to 70) to hypertrophic level (70 to 100), with the algae scum attribute based on the TSI category of Carlson and Simpson (1996). Resultant Chla and SD at 60 simultaneously measured points showed a significant relationship ($R^2$ = 0.60) following an exponential curve (Fig. 2(a)), illustrating a high dependence of the water clearance (or turbidity) on the abundance of phytoplankton in water. However, the correlation of $TSI_{Chla}$ and $TSI_{SD}$ was not strong ($R^2$ =

**Table 2** Field measured water quality parameters, including the Secchi Depth (SD), chlorophyll-a concentration (Chla) and the trophic state index (TSI) of studied lakes in Hanoi (Vietnam)

| Date | Lake | Sample No. | SD/m | Chla/(μg·L$^{-1}$) | TSI |
|---|---|---|---|---|---|
| June 1st 2016 | West, Ba Mau, Bay Mau, Nam Dong, Dong Da, Giang Vo, Linh Dam, Nghia Tan, Thien Quang, Thu Le | 42 | 0.05 − 0.51 | 48.7 − 541 | 69 − 100 |
| October 7th 2016 | Hoan Kiem, West, Van Quan, Bay Mau, Dong Da, Giang Vo, Linh Dam, Nghia Tan, Thien Quang | 30 | – | 84.6 − 273.9 | 76 − 86 |
| April 1st 2017 | Linh Dam | 12 | 0.21 − 0.53 | 30.5 − 98.74 | 67 − 79 |
| June 4th 2017 | Van Quan | 6 | 0.03 − 0.07 | 358.1 − 566.8 | 93 − 100 |
| June 26th 2019 | Thu Le, Van Quan | 16 | 0.15 − 0.49 | – | 70 − 88 |
| August 13th 2019 | West | 15 | – | 118 − 270.6 | 77 − 86 |
| December 3rd 2019 | Van Quan, Dong Mo | 17 | 0.15 − 1.40 | – | 55 − 87 |

Notes: "–" means no data; "…− …" is from minimum to maximum.

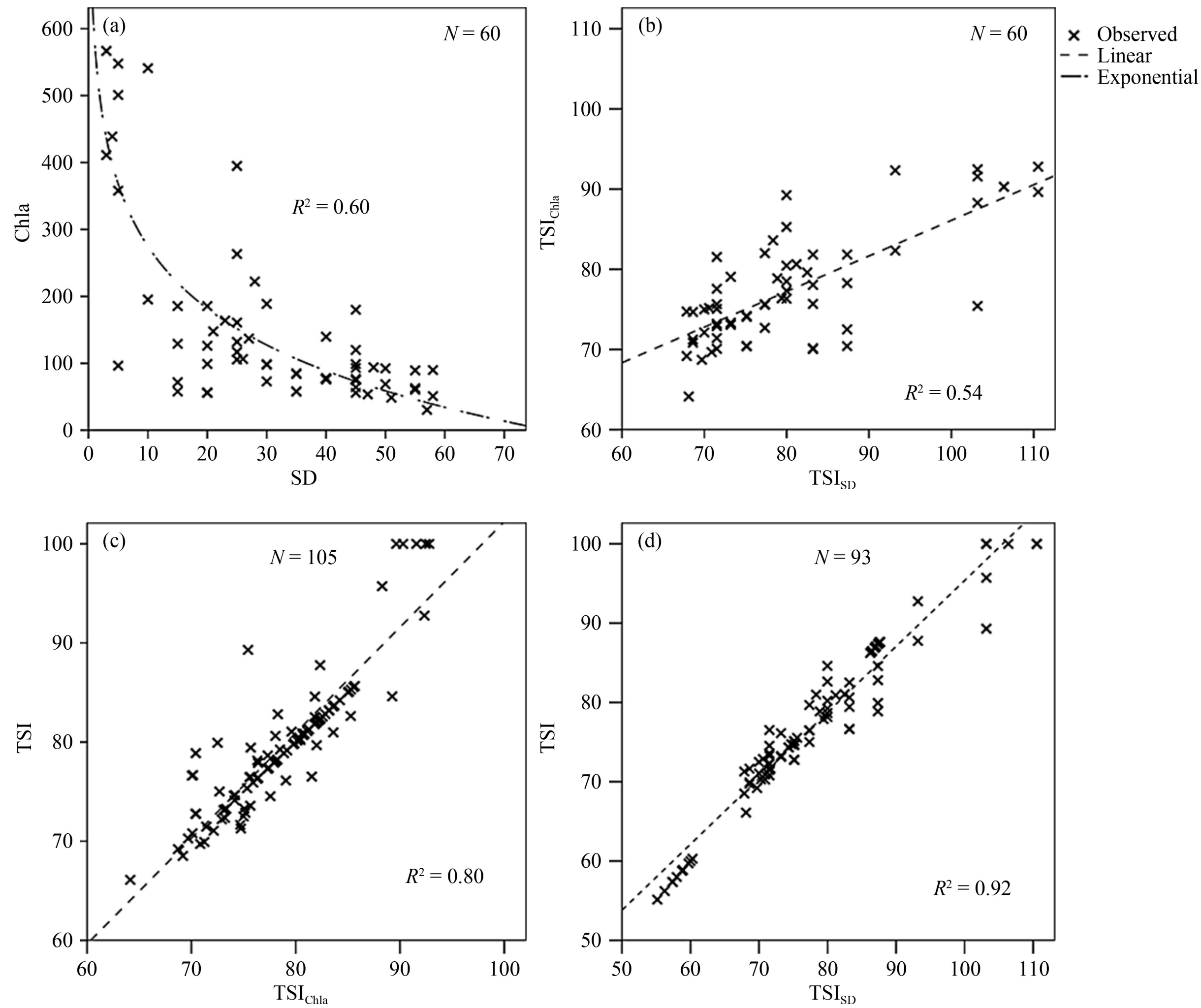


**Fig. 2** Correlations between (a) *in situ* chlorophyll-a concentration (Chla, μg/L) and Secchi Depth (SD, cm); (b) trophic state index (TSI) calculated from *in situ* Chla ($TSI_{Chla}$) and TSI calculated from *in situ* SD ($TSI_{SD}$); (c) and (d) *in situ* TSI and $TSI_{Chla}$ and $TSI_{SD}$. These relationships indicate a stronger dependence of *in situ* TSI on SD than Chla (c, d). The TSI value ranges from 55 to 100, corresponding to the trophic levels from eutrophic to super-hypertrophy (Carlson and Simpson, 1966).

0.54, Fig. 2(b)); nevertheless the final *in situ* TSI was highly correlated with both $TSI_{Chla}$ and $TSI_{SD}$ (Figs. 2(c) and 2(d), $R^2$ = 0.80 and 0.92, respectively). In particular, *in situ* TSI depended more strongly on $TSI_{SD}$ than $TSI_{Chla}$ at values ranging from 50 to 60 and 90 to 100 (Figs. 2(c) and 2(d)), suggesting that the SD measurement should be carried out simultaneously with Chla determination to assess the lake trophic level.

The lowest TSI values of lakes in Hanoi urban were recorded in Linh Dam Lake in April 2017, ranging from 66 to 72. The highest value of TSI was obtained in Giang Vo Lake in June 2016 and Van Quan Lake in June 2017 (from 90 to 100), corresponding to a Chla value that reached over 500 μg/L, and floating scum was observed (Fig. 3). These *in situ* TSI data agreed with other domestic studies in identifying the trophic state of lakes in Hanoi urban areas based on total phosphorus concentration or other indicators (Nguyen et al., 2016; Hoang et al., 2017; Thuy et al., 2017). Several lakes, i.e., Van Quan Lake, Giang Vo Lake, Hoan Kiem Lake, and West Lake, had a very high level of Chla (> 200 μg/L) in water and therefore were sensitive to algae blooms and scums, which had recently been recorded.

General features of measured water reflectance, $\rho_\omega(\lambda)$, within the range of 400–900 nm of eight points representing optical water features of eight lakes in Hanoi (Fig. 1) are shown in Fig. 3. Water reflectance spectra of these lakes confirmed the high trophic level of the waters with a very strong peak appearing near 709 nm (Schalles, 2006; Matthews and Bernard, 2013). The horizontal bias of peaks of spectra in the green region shows a difference in dominated algae taxa among these lakes (Schalles, 2006). At very high values of TSI (e.g., TSI of Van Quan Lake = 100 and TSI of Ba Mau Lake = 87), $\rho_\omega(\lambda)$ in the green region showed a lower value than in other waters with lower TSI values (Fig. 3). Conversely, at TSI values lower than 83, $\rho_\omega(\lambda)$ in the green region demonstrated an increasing trend in agreement with the increase in TSI. Similar trends were observed in the red region corresponding to the L8 red band of 640–670 nm. The

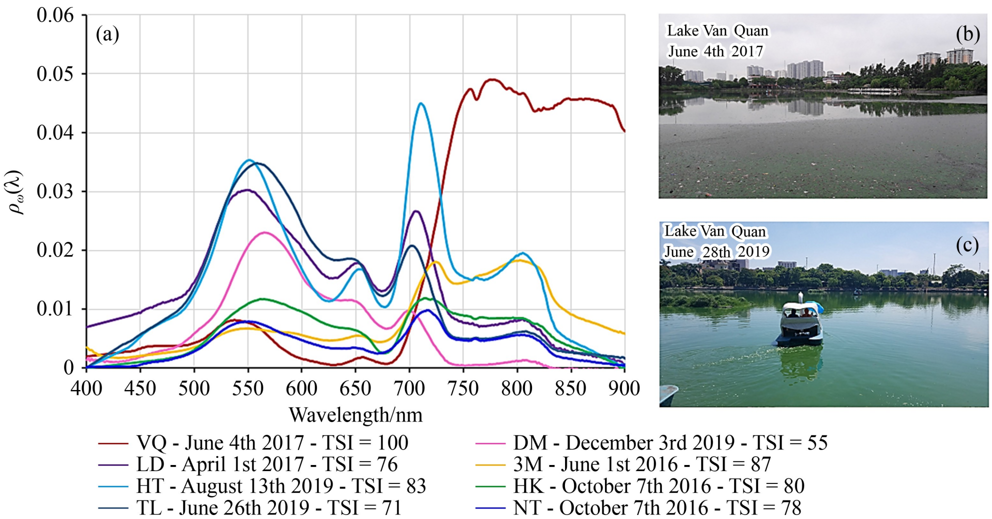


**Fig. 3** (a) Features of water reflectance spectra of studied lakes and TSI calculated from measured points; (b) and (c) photos of algae scums and floating in Van Quan Lake in June 2017 and 2019. VQ: Van Quan Lake; LD: Linh Dam Lake; HT: West Lake, TL: Thu Le Lake; DM: Dong Mo Lake; 3M: Ba Mau Lake; HK: Hoan Kiem Lake; NT: Nghia Tan Lake.

most significant relationship between $\rho_\omega(\lambda)$ and TSI was observed in the region corresponding to the L8 NIR band (850–880 nm) with the Pearson correlation coefficient ($R$) equal to 0.80, suggesting that the L8 NIR band is applicable for estimating TSI.

### 3.2 Performance of L8-LaSRC and L8PAR

Assessing lakes' trophic state is a critical task in urban environmental management at the local level. The utility of L8 data for determining and monitoring lakes' trophic state provides economic and practical efficiency if the data are easy to access and process. Since atmospheric correction is a necessary procedure in remote-sensing-based water retrievals, the use of readily available, processed data, such as L8-LaSRC and L8PAR, is a significant advance due to their convenience for water management at the local level. However, the performance of L8-LaSRC and L8PAR should be evaluated to select favorable data for use at the local level.

Figure 4 shows a visual comparison of L8-LaSRC and L8PAR for the L8 scene acquired on August 13th 2019 in ten urban districts of Hanoi city. The RGB image of the L8-LaSRC false-color composition (band 7, band 5, band 3) and the band 9 (cirrus) image are shown in Figs. 4(a) and 4(b), respectively, illustrating no-cloud cover over the studied lakes. Water surfaces of 12 studied lakes in the Hanoi urban areas are displayed clearly in association with the surrounding landscape. The retrieval of $R_{rs}(\lambda)$ from L8PAR is shown in Fig. 4(b), presenting a large area of missing $R_{rs}(\lambda)$ data for 12 studied lakes, with negative values for all dark-colored pixels. Positive values were only found in areas marked in yellow. Indeed, Fig. 4 shows poor performance of L8PAR data for water retrievals in small and shallow lakes, which are common features of lakes in Hanoi's urban areas.

Figure 5(a) shows the status of L8PAR data for West Lake on August 13th 2019. Accordingly, there were 13 points out of a total of 15 points of *in situ* measurement out of areas with positive values. L8PAR values extracted from these 13 points were flattened over all four bands of L8-visible bands (bands 1 to 4) and were "−9999", as presented in all dark pixels. Only two pixels corresponding to two measured points (HT9 and HT12) had positive values, which equaled 0 for the bands 1, 2, and 4 in both pixels. The values of band 3 for these two pixels were 0.011 and 0.024, respectively, and were lower than *in situ* $\rho_w$ (533–590) shown in Fig. 6(a).

Overall, the present version of L8PAR is not suitable for water retrievals in inland lake waters because of marking almost all of the lake surface as "dark pixels", which contain only negative values over the whole four bands (visible and NIR bands) as reported by Ogashawara et al. (2020) and may be more favorable for water retrievals in coastal waters (Nazeer et al., 2020).

L8-LaSRC provides data for all sizes of water surface, from the scale of several-pixels to large lakes (Fig. 4(a)); therefore, it can be used for water retrievals in small urban lakes. However, LaSRC was shown to overestimate in retrieving $R_{rs}(\lambda)$ from the NIR band (band 5) over water surfaces because the effect of the reflected skylight was not accounted for in the algorithm (Bernardo et al., 2017). Figure 6 shows the difference of L8-LaSRC-based reflectance spectra features compared to the *in situ* reflectance spectra. The *in situ* reflectance spectra in Figs. 6(a) and 6(b) demonstrate the similarities in all 15 measured points, while the L8-LaSRC reflectance spectra presented bias over each point. A large difference between *in situ* data (Fig. 6(b)) and L8-LaSRC data was observed at band 5 (B5): *in situ* values corresponding to B5 are lower than those of B2, B3, and B4, but L8-LaSRC B5 values are higher than B4, B2, and B3 (in several points) values. In this sense, the large deviations between the remote-sensing-based water optical features and on-surface water optical features should be

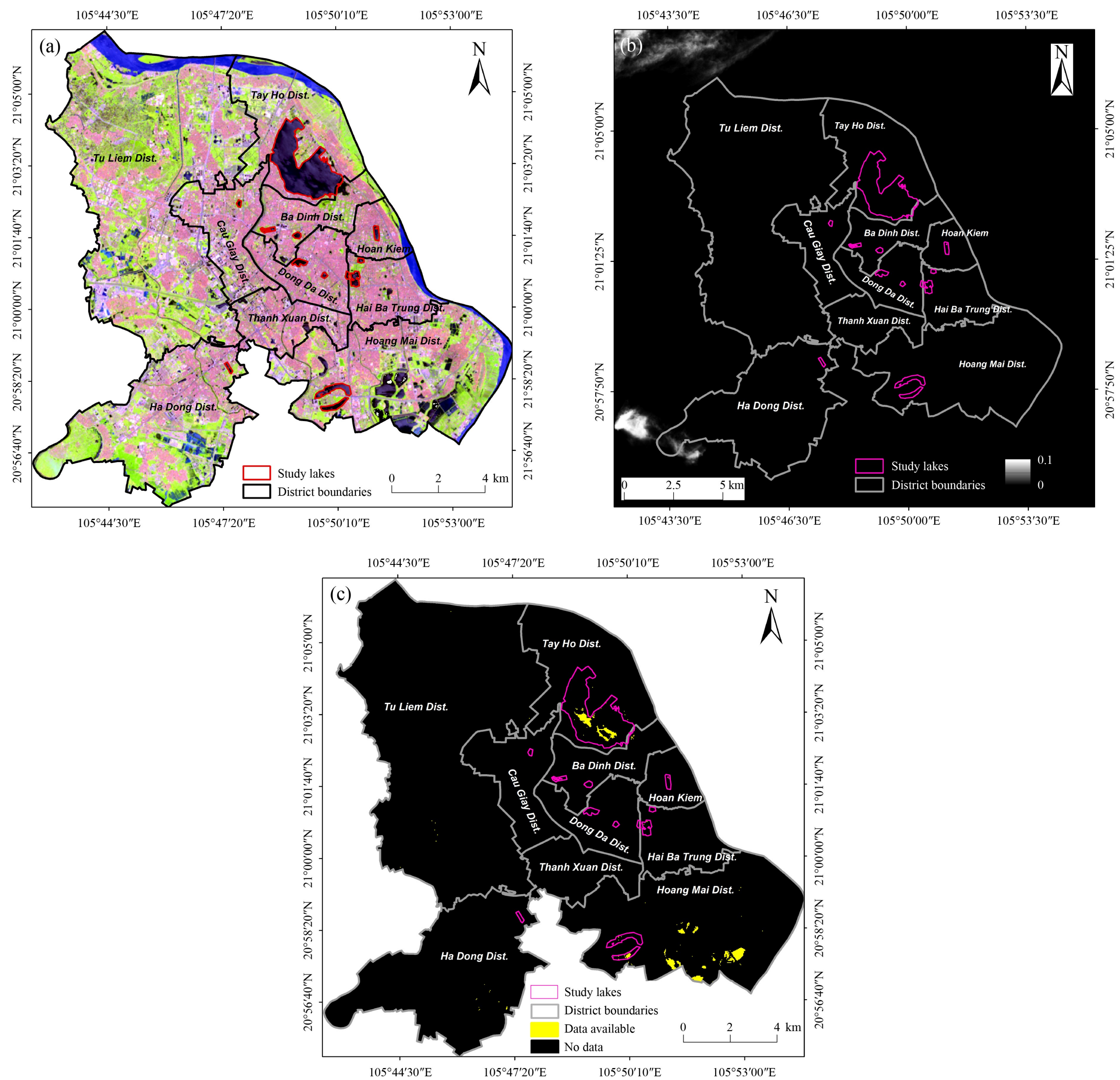


**Fig. 4** Landsat 8 (L8) data acquired on August 13th 2019 in ten urban districts of Hanoi city: (a) a RGB composite image (band 7, band 5, band 3) of Landsat 8 processed by the the Land Surface Reflectance Code (L8-LaSRC); (b) the band 9 (cirrus) image presents no-cloud cover over the studied lakes; (c) a RGB composite image (band 3, band 2, band 1) of Level 2 Flag from the Landsat 8 Provisional Aquatic Reflectance Product (L8PAR) with the yellow marks areas in (a) indicating the missing data of L8PAR in most studied lakes.

considered when applying bio-optical or analytical algorithms for water retrievals using L8-LaSRC data. In this case, the use of an empirical algorithm is more suitable for water retrievals than bio-optical or analytical algorithms.

## 3.3 Empirical model for estimating TSI from L8-LaSRC

For better long-term monitoring of TSI, a reliable empirical model for estimating TSI from L8-LaSRC should be developed based on multi-date measurements and a wide range of TSI values. First, the cross relationships of *in situ* TSI at 138 measured points and the corresponding L8-LaSRC-derived $R_{rs}(\lambda)$ were investigated. The result shows that TSI was significantly correlated to B5 ($R$ = 0.67) but uncorrelated to the other bands (B1: $R$ = 0.08; B2: $R$ = 0.00; B3: $R$ = 0.12; B4: $R$ = 0.13). Based on the feature of water reflectance spectra mentioned in Section 3.1, ratios of the NIR band (B5) versus two other visible bands the red band (B4) and the green band (B3) were also investigated for the correlation with *in situ* TSI. Two blue bands of L8-LaSRC (B1 and B2) were warned not to be used in users' analysis by the LaSRC developers because these bands have already been used within the algorithm to perform aerosol inversion tests (USGS, 2020a); therefore, they were not included in the investigation. Strong correlations between TSI and

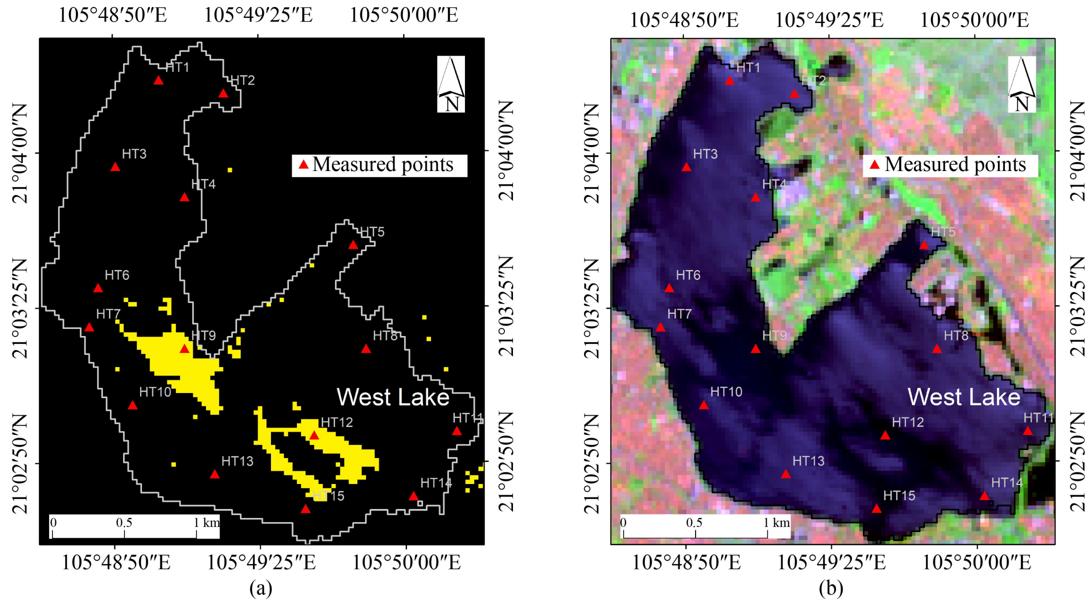


**Fig. 5** Landsat 8 (L8) data acquired on August 13th 2019 over West Lake in the Hanoi urban areas and location of 15 radiometric measuring points: (a) an RGB composite image (band 3, band 2, band 1) of Level 2 Flag from L8PAR; (b) an RGB composite image (band 7, band 5, band 3) of L8-LaSRC. Several yellow areas in (a) provided positive values over four L8 bands in visible and near-infrared regions (band 1 to band 4), while the dark pixels gave negative values to the whole four bands, indicating the missing data of L8PAR in most studied lakes even the L8 data was collected under the cloud-free condition for that date.

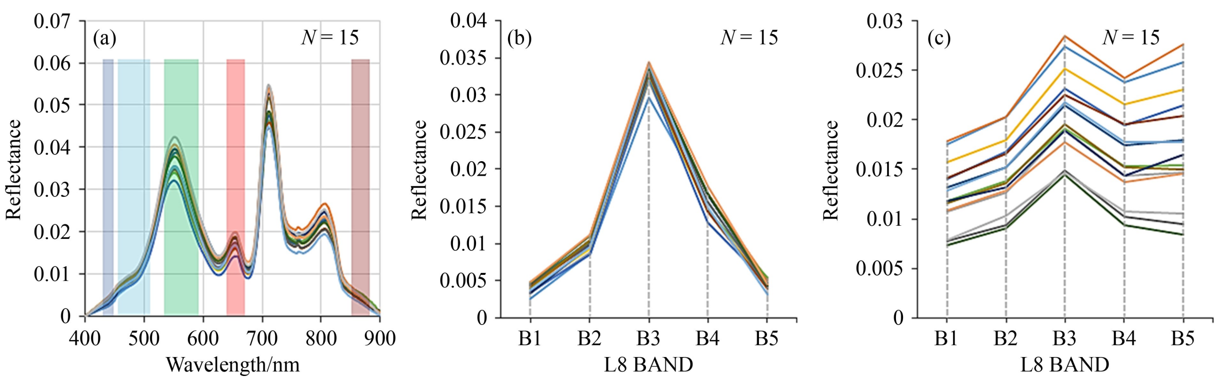


**Fig. 6** Difference between *in situ* reflectance spectra and water surface reflectance spectra extracted from the L8 scene acquired on August 13th 2019 after correcting using LaSRC: (a) *in situ* water reflectance spectra, $\rho_\omega(\lambda)$, overlaid L8/OLI band responses measured at 15 points in West Lake with the locations as shown in Fig. 5; (b) simulated *in situ* $\rho_\omega(\lambda)$ for L8/OLI band values based on the band-average relative spectral responses (Barsi et al., 2014) shown in (a); (c) water surface reflectance spectra extracted from L8-LaSRC pixels corresponding to 15 measured points. B1 to B5 are L8 band in the visible and NIR regions.

B5/B3 ($R$ = 0.77) and B5/B4 ($R$ = 0.72) were observed. The result from curve-fitting analysis of TSI with B5/B3 and B5 demonstrated the best fit of the logarithmic curve for describing the cross-relationship between TSI and B5/B3 (Fig. 7(a)), while a linear line is the best fit for describing the relationship between TSI and B5 (Fig. 7(b)). The highest value of the determination coefficient of the relationship between TSI and B5/B3, $R^2$ = 0.65, suggested that this band ratio is favorable for estimating TSI from L8-LaSRC. B5 data, however, showed a significant correlation with TSI ($R^2$ = 0.45); nevertheless B5 was not suitable for estimating the index because of the strong deviation of the data due to the interference of the effect of the reflected skylight (Fig. 7(b)). Band-ratioing has been proven as a method that helps reduce the effect of the atmosphere on the water reflectance signals (Ha et al., 2017b). Therefore, the use of the band ratio model (B5/B3) is better than a single-band model (B5) in reducing the effect of reflected skylight.

Accordingly, TSI can be estimated from L8-LaSRC by the equation for the logarithmic curve shown in Fig. 7(a):

$$\mathrm{TSI} = 21.46 \cdot \ln\left(\frac{\mathrm{B5}}{\mathrm{B3}}\right) + 79.66, \tag{5}$$

where TSI is a non-unit quantity, B5 and B3 is $R_{rs}(\lambda)$, derived from the NIR band (B5) and the green band (B3), of L8 after correction by LaSRC.

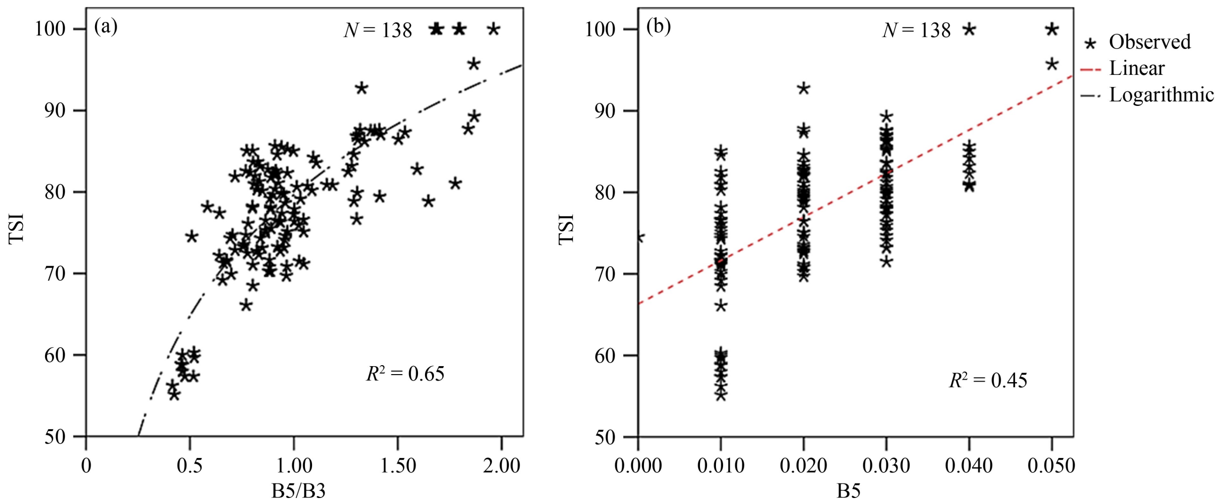


**Fig. 7** The best-fit curve analysis of the relationship between (a) *in situ* TSI and reflectance ratio of the NIR band (B5) versus the green band (B3) of L8-LaSRC data; (b) *in situ* TSI and L8-LaSRC-derived B5 reflectance. This relationship demonstrated a high potential of B5/B3 for estimating TSI of lakes in the Hanoi urban area.

Performance of Eq. (5) in estimating TSI was evaluated using 28 Chla-measured points in small lakes and ponds in the Hanoi urban area by CECR in the first week of July 2015 (CECR, 2015). Equation (5) was applied to L8-LaSRC of the scene acquired on July 1st 2015 over the Hanoi urban area to estimate TSI for 28 pixels corresponding to 28 measured points (Fig. 8(a)). The validation result shown in Fig. 8(b) demonstrates a good match of estimated TSI and *in situ* TSI using Eq. (5). The standard error of the estimates (root mean squared error (RMSE) = 6.6) was smaller than the interval of the TSI category (Carlson and Simpson, 1996), confirming the appropriateness of Eq. (5) for estimating TSI in small and shallow lakes like those in Hanoi's urban area.

## 3.4 Changes in trophic state of lakes in Hanoi's urban area

Figure 9 demonstrates the application of Eq. (5) for estimating TSI of 25 lakes in the Hanoi urban areas from L8-LaSRC of two scenes acquired on July 1st 2015 and June 28th 2020. In the figure, large changes of TSI were observed in West Lake, Hoan Kiem Lake, and Dinh Cong Lake: mean TSI values of West Lake increased from 65 to 70 (corresponding to a highly eutrophic level) in early July 2015 to 75–80 (corresponding to hypertrophic level) in late June 2020, but the mean TSI value of Dinh Cong Lake decreased from over 90 in July 2015 to 80–85 in June 2020. Although most lakes in the Hanoi urban area were chemically treated for organic pollution by the city government from 2016 to 2019, the increasing trend in

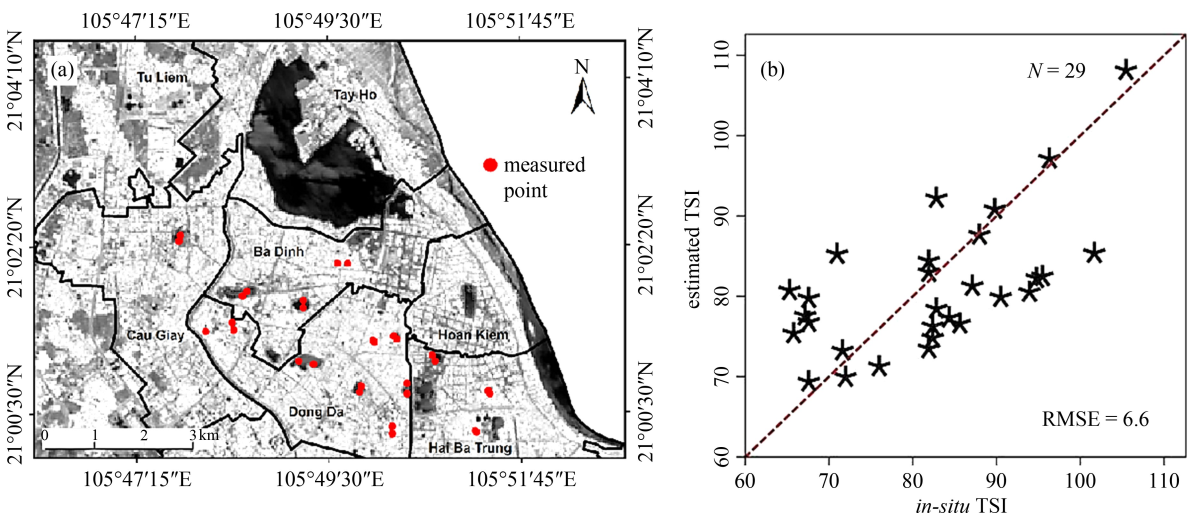


**Fig. 8** (a) Locations of 29 Chla-measured points in small lakes and ponds in Hanoi urban area by Center for Environment and Community Research (CECR) (2015) used for validating the Eq. (5); (b) result of matched-up validation between *in situ* TSI calculated from Chla at 29 points shown in (a) and estimated TSI from L8-LaSRC data by Eq. (5) compared to the 1:1 reference line (the red dashed line).

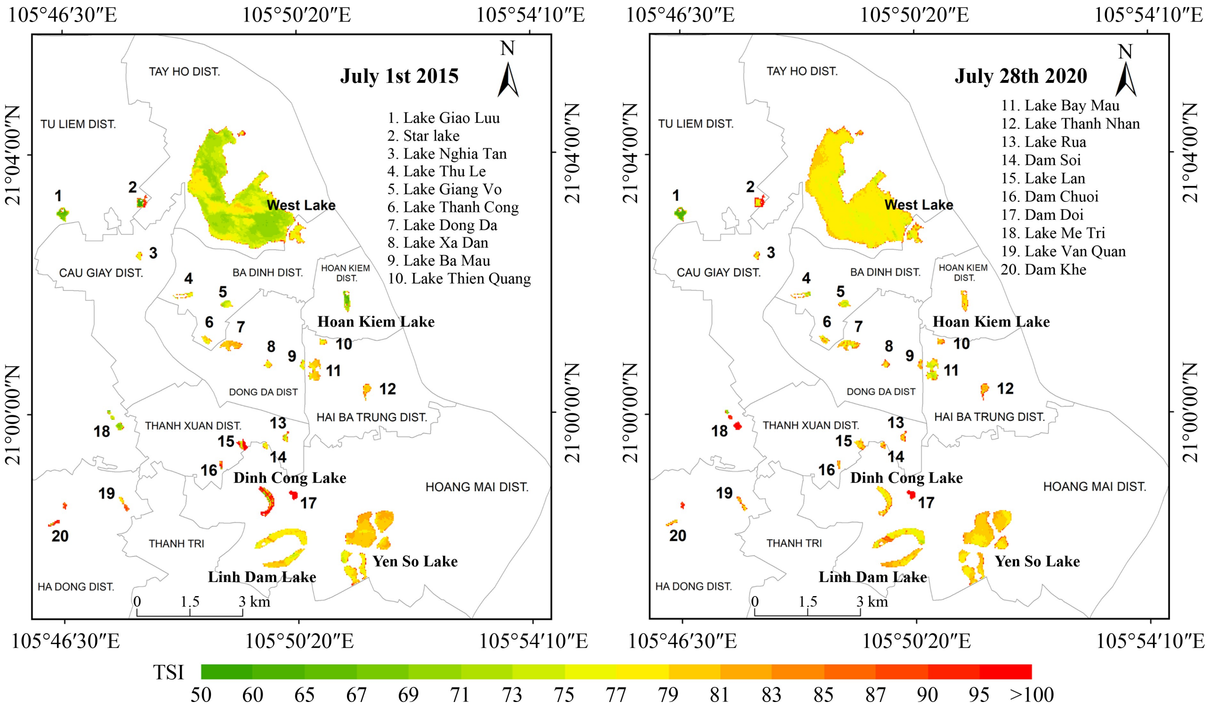


**Fig. 9** Change in TSI of lakes in Hanoi urban area after five years (from 2015 to 2020).

TSI has remained and been observed in large lakes such as West Lake, Linh Dam Lake, Yen So Lake, and Hoan Kiem Lake. In several small lakes, such as Dong Da Lake, Bay Mau Lake, Lan Lake, and Dinh Cong Lake, TSI demonstrated a decreasing trend but still corresponded to the hypertrophic level. Figure 9 suggests that TSI changes at two time points (corresponding to the 5-year interval as published by CECR (2015)) were unable to reflect the TSI dynamic and driving factors affecting the changing trend. Long-term monitoring with a shorter time interval should be conducted to understand the eutrophication driving forces and the efficiency of protective measures. For instance, a year-long period of monitoring at a lake scale of West Lake in the early summer every year from 2015 to 2020 (Fig. 10) provided more detailed information on the dynamics of TSI and associated factors.

Focusing on West Lake, the change of TSI of this lake over 5 years from 2015 to 2020 is shown in Fig. 10. Estimated TSI from L8-LaSRC of West Lake in early summer (June–July) has varied from 65 to 70 in July 2015 (corresponding to highly eutrophic level) to 85–90 in June 2019 (corresponding to highly eutrophic level to super-hypertrophic level) and was 75–80 in this year summer (June 2020). It was acknowledged that high temperature leads to increased soluble phosphate concentration in the water, leading to an increase in algae blooms and floating plants, particularly in shallow lakes (Feuchtmayr et al., 2009). The cases of West Lake in June 2019 and 2017 were prime examples of this point. According to Vietnam Institute of Meteorology, Hydrology and Climate Change (2019), the mean temperature in June 2019 was 0.7°C to 1°C higher than that of June in the other years, during which several heatwaves occurred. During the first week of June 2017 (precisely from June 2nd 2018 to June 5th 2018), a historical heatwave occurred in Hanoi, with the highest temperature reaching 42.5°C on June 4th 2018 (Wunderground, 2017). Consequently, phytoplankton in West Lake grew excessively, and algae blooms occurred in several areas along the shoreline of West Lake, leading to increased TSI (Fig. 10). Conversely, during the first week of June 2018, lakes in Hanoi were diluted by rainwater, leading to decreased TSI.

## 4 Discussion

Literature review results show that the lake trophic index, TSI, was often computed indirectly from remote sensing data, particularly from estimated Chla or SD (Odermatt et al., 2012; Buttand and Nazeer, 2015; Watanabe et al., 2015). The uncertainty of estimated TSI based on the indirect approach suggested a direct approach for rapidly monitoring and mapping the TSI (Shi et al., 2019). If the use of the analytical algorithm proposed by Shi et al. (2019), based on the relationship of TSI with the absorption coefficient at 440 nm (L8 band 1), was found to be limited for estimating TSI in lakes with a high concentration of CDOM, which is a common feature of small and shallow lakes in the tropical region such as lakes in the Hanoi urban areas, and the machine learning model, the radial basis function (RBF) neural network, proposed by Zhou et al. (2019) to estimate TSI directly

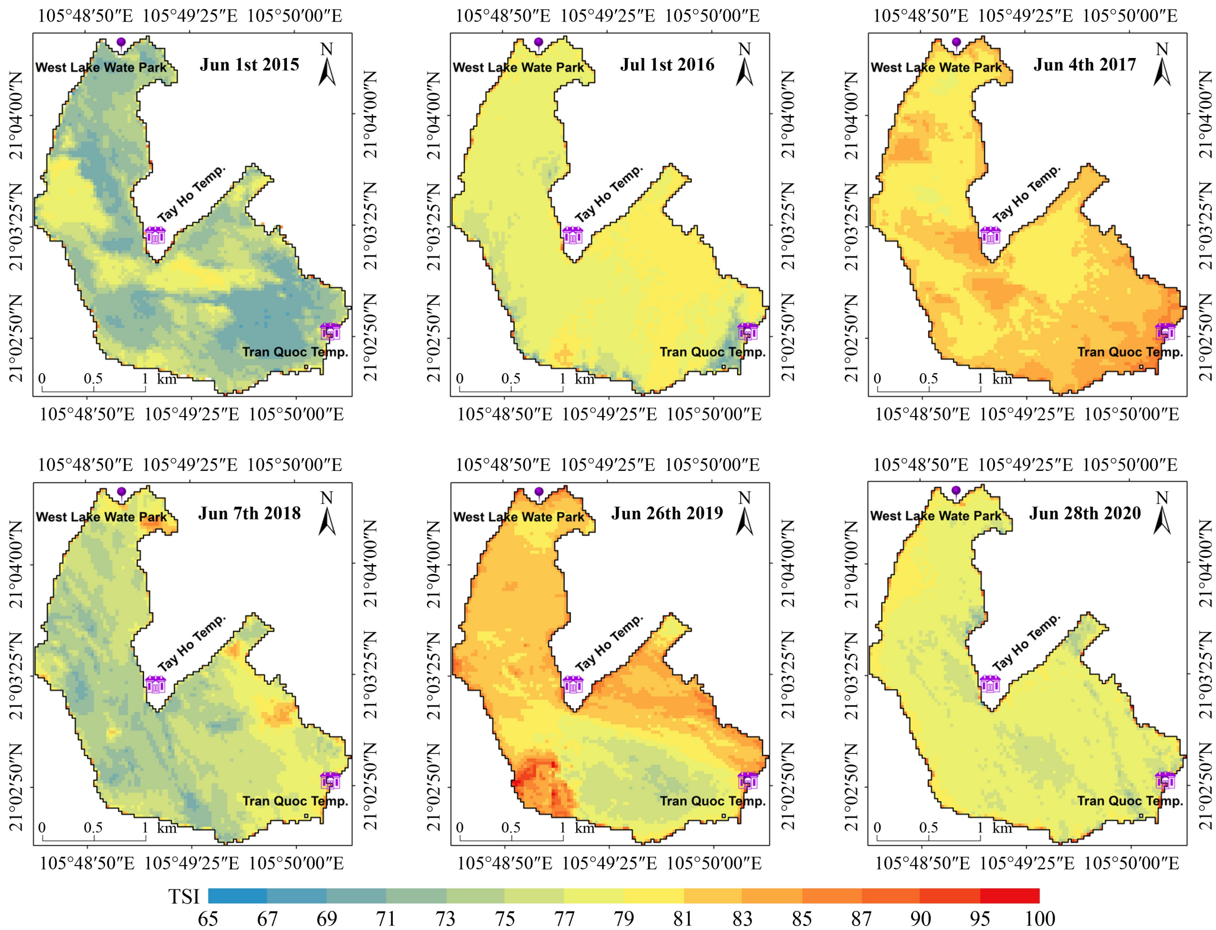


**Fig. 10** L8-LaSRC-derived TSI changes in West Lake in early summers of 2015, 2016, 2017, 2018, 2019, and 2020.

from L8 data was challenged from the model's applicability in a broad region with various water trophic levels and seasonal fluctuation of TSI, then our empirical model was validated with reasonable error (RMSE = 6.6, corresponding to 8% of the *in situ* TSI mean) using the TSI measured by the local community, confirming the appropriateness of the model for monitoring the TSI of lakes in Hanoi.

Indeed, within the Hanoi urban areas in particular and in urban tropical regions in general, lakes have been exposed to the acceleration of eutrophication due to anthropogenic pollution and high temperature derived from urbanization. Therefore, the TSI of lakes often ranges from eutrophic level (TSI = 50–60) to hypertrophic level (TSI > 80), even with algae blooms (TSI > 90). The empirical model proposed in this study based on the *in situ* TSI range of 55 to 100 (corresponding to SD < 2 m) is suitable for monitoring the trophic state of urban lakes where lakes often range from 2 to 4 m depth. The input data set for building the proposed model was collected in many lakes scattered over the region and multiple dates over three years (2016 to 2019), ensuring the diversity of trophic levels and the seasonal variations of *in situ* TSI.

In this study, the effect of suspended non-algae particles (NAP) in the water on the retrieved L8 reflectance has not been accounted for because algae particles were predominant in the studied lake waters, which was evidenced through a strong correlation of Chla and SD ($R$ = −0.77). If the effect of NAP is too large, leading to the correlation of Chla and SD becoming smaller than the correlation of NAP and SD, then the proposed empirical model may not be proper for estimating the TSI. Furthermore, *in situ* data should be collected in water at oligotrophic and mesotrophic levels to provide a lower bound for the model for a broader application to lakes and ponds in Vietnam and the tropical region. Presently, there are no reports on the oligotrophic waters in Vietnam (with SD > 8 m), and mesotrophic waters such as Lake Ba Be (Ha et al., 2017b) and Thac Ba Reservoir (Vinh et al., 2019) should be investigated for the application to lakes over the whole country.

The annual dynamic of TSI of West Lake (Fig. 10) demonstrated the fluctuations of TSI and the effect of air temperature on the trophic lake state. It is suggested that the monitoring program for the trophic lake state should be carried at monthly or seasonal scales in cooperation with a cross-analyses of main influencing factors, such as temperature, sunshine hours, precipitation, and total nutrient load by watershed (Chen et al., 2020). Urban shallow lakes with their vital role in support of biodiversity in the Hanoi urban areas, as well as over the world, are becoming vulnerable to eutrophication due to current warming and urbanization, which require an effective strategy and protective measures.

L8-LaSRC data are easily accessible and usable; however, it is still limited in spatial resolution for urban lake monitoring. While Lillesand et al. (1983) recommended not to use Landsat MSS with a spatial resolution of 60 m for bodies of water smaller than 12 ha, presently, lakes of 12 ha size can provide data in more than a hundred pixels of L8 for TSI assessment. However, optical remote sensing data such as L8 are often limited by cloud cover when acquired over tropical regions like Hanoi (Vietnam). In addition, a revisit time of 16 days of L8 is inadequate for monthly monitoring. More investigations and exploitations on other open data sources such as Sentinel 2A and 2B should be carried out for better water management.

## 5 Conclusions

This study established an empirical model for directly estimating the TSI of lakes from L8-LaSRC data using *in situ* data of 138 points measured in 13 lakes in Hanoi on seven L8 dates in the period of 2016–2019. With the value ranging from 55 to 100, corresponding to eutrophic to hypertrophic levels, TSI of lakes in Hanoi was strongly correlated ($R^2$ = 0.65) with the spectral ratio of L8-LaSRC-derived B5/B3 (ratio of the NIR band versus the green band) and can be reasonable estimated from this ratio by a logarithmic function (Eq. (5)). The validation results using *in situ* data published by CECR (2015; $N$ = 28) demonstrated the appropriateness of the proposed model (RMSE = 6.6) for estimating TSI of lakes in Hanoi's urban area, which are commonly classified into highly eutrophic to hypertrophic states. The approach was applied in six selected L8/OLI scenes acquired in six different summers (2015, 2016, 2017, 2018, 2019, and 2020) to observe the changes in TSI of 25 lakes in the Hanoi urban areas for five years (2015 and 2020) and of TSI of West Lake (in Hanoi, Vietnam) every summer. This was done in order to discuss the suitable time interval for TSI monitoring and forces driving the increasing trend in TSI. More *in situ* data should be collected in oligotrophic and mesotrophic lakes to complete the model for a wider application.

In this study, we also evaluated the performance of L8PAR data for small and shallow inland lakes using 15-point *in situ* reflectance data measured in West Lake. The results show that L8PAR was inappropriate for monitoring water quality in small shallow inland lakes for visual interpretation and data extraction. L8-LaSRC provides better data under the no-cloud cover condition, and such data are better for establishing empirical models than for developing semi-analytical algorithms. Eq. (5) with L8-LaSRC data can be applied to monitoring the TSI of lakes in tropical regions with lakes similar to those in Hanoi's urban areas.

The results demonstrated the sufficient radiometric performance of L8-LaSRC to be of potential use for monitoring freshwater lakes untroubled by atmospheric correction issues. With a significant advantage in accessing and processing the data, L8-LaSRC opens up an excellent opportunity for water quality monitoring of freshwater lakes at regional and local levels, particularly in monitoring the trophic state of urban lakes intensely threatened by eutrophication and algae blooms.

**Acknowledgments** This research was funded by Vietnam Academy of Science and Technology (No.VAST01.04/19-20). The authors thank the US Geological Survey and NASA for providing the LaSRC and other Landsat data. Many thanks for the kind support from Dr. Michael Parsons, Policy Adviser to the Minister of Vietnam Ministry of Natural Resources and Environment, in the language editing of the paper.

## References

Allam M, Yawar Ali Khan M, Meng Q (2020). Retrieval of turbidity on a spatio-temporal scale using Landsat 8 SR: a case study of the Ramganga River in the Ganges Basin, India. Appl Sci (Basel), 10(11): 3702

APHA (1998). Standard Methods for the Examination of Water and Wastewater Analysis. Washington DC: American Public Health Association

Barsi J A, Lee K, Kvaran G, Markham B L, Pedelty J A (2014). The spectral response of the Landsat-8 operational land imager. Remote Sens, 6(10): 10232–10251

Bernardo N, Watanabe F, Rodrigues T, Alcântara E (2017). Atmospheric correction issues for retrieving total suspended matter concentrations in inland waters using OLI/Landsat-8 image. Adv Space Res, 59(9): 2335–2348

Birch S, McCaskie J (1999). Shallow urban lakes: a challenge for lake management. Hydrobiologia, 395: 365–378

Boucher J, Weathers K C, Norouzi H, Steele B (2018). Assessing the effectiveness of Landsat 8 chlorophyll a retrieval algorithms for regional freshwater monitoring. Ecol Appl, 28(4): 1044–1054

Buma W G, Lee S I (2020). Evaluation of Sentinel-2 and Landsat 8 images for estimating chlorophyll-a concentrations in Lake Chad, Africa. Remote Sens, 12(15): 2437

Butt M J, Nazeer M (2015). Landsat ETM+ Secchi Disc Transparency (SDT) retrievals for Rawal Lake, Pakistan. Adv Space Res, 56(7): 1428–1440

Carlson R E (1977). A trophic state index for lakes. Limnol Oceanogr, 22(2): 361–369

Carlson R E, Simpson J (1996). A coordinator's guide to volunteer lake monitoring methods. North Amer Lake Manag Soc, 96: 305

Center for Environment and Community Research (CECR) (2010). Hanoi Lakes Report 2010. Hanoi, Vietnam: Publishing Company of Women

Center for Environment and Community Research (CECR) (2015). Hanoi Lakes Report 2015. Hanoi, Vietnam: Publishing Company of

Women
Chang N B, Imen S, Vannah B (2015). Remote sensing for monitoring surface water quality status and ecosystem state in relation to the nutrient cycle: a 40-year perspective. Crit Rev Environ Sci Technol, 45(2): 101–166
Chen Q, Huang M, Tang X (2020). Eutrophication assessment of seasonal urban lakes in China Yangtze River Basin using Landsat 8-derived Forel-Ule index: a six-year (2013-2018) observation. Sci Total Environ, 745: 135392
Chen W, Zhang T, Guan L (2018). Radiation transfer in the ocean and ocean color
Dave A, Chaplot N, Chander S, Gujarati A, Singh R P, Patel H M, Patel U D (2019). Assessment of Water Quality Parameters for Some Inland Water Bodies of Western India Using Landsat 8 Data. In: World Environmental and Water Resources Congress 2019: Groundwater, Sustainability, Hydro-Climate/Climate Change, and Environmental Engineering. Reston: American Society of Civil Engineers, 98−107
Feuchtmayr H, Moran R, Hatton K, Connor L, Heyes T, Moss B, Harvey I, Atkinson D (2009). Global warming and eutrophication: effects on water chemistry and autotrophic communities in experimental hypertrophic shallow lake mesocosms. J Appl Ecol, 46(3): 713–723
Fuller L M, Jodoin R S (2016). Estimation of a Trophic State Index for selected inland lakes in Michigan, 1999–2013. In: U.S. Geological Survey Scientific Investigations Report 2016−5023
Gholizadeh M H, Melesse A M, Reddi L (2016). A comprehensive review on water quality parameters estimation using remote sensing techniques. Sensors (Basel), 16(8): 1298
Ha N T T, Canh B D, Thao N T P, Nhi B T (2016). First experience in modeling spatial distribution of chlorophyll-a concentration and TSI in the West Lake Water using Sentinel-2A image. VNU J Sci: Earth Environ Sci, 32: 121–130
Ha N T T, Koike K, Nhuan M T, Canh B D, Thao N T P, Parsons M (2017a). Landsat 8/OLI two bands ratio algorithm for chlorophyll-a concentration mapping in hypertrophic waters: an application to West Lake in Hanoi (Vietnam). IEEE J Sel Top Appl Earth Obs Remote Sens, 10(11): 4919–4929
Ha N T T, Thao N T P, Koike K, Nhuan M T (2017b). Selecting the best band ratio to estimate chlorophyll-a concentration in a tropical freshwater lake using sentinel 2A images from a case study of Lake Ba Be (Northern Vietnam). ISPRS Int J Geoinf, 6(9): 290
Han V T, Ha N T T, Thao N T P, Khanh D T M (2017). Monitoring the trophic state index of Lake Linh Dam using Landsat 8 Imagery. J Mining Earth Sci, 58(3): 42–50
Hoang T H T, Van A D, Nguyen H T T (2017). Driving variables for eutrophication in lakes of Hanoi by data−driven technique. Water Environ J, 31(2): 176–183
Jiang D, Matsushita B, Setiawan F, Vundo A (2019). An improved algorithm for estimating the Secchi disk depth from remote sensing data based on the new underwater visibility theory. ISPRS J Photogramm Remote Sens, 152: 13–23
Kuhn C, Matos Valerio A, Ward N D, Loken L C, Sawakuchi H O, Kampel M, Richey J E, Stadler P, Crawford J, Striegl R G, Vermote E, Pahlevan N, Butman D E (2018). Assessment of atmospheric correction methods for Landsat-8 and Sentinel-2 over large rivers. In: American Geophysical Union Fall Meeting U12B–08, Washington D.C.
Kumar Jally S, Kumar Mishra A, Balabantaray S (2020). Estimation of trophic state index of Chilika Lake using Landsat-8 OLI and LISS-III satellite data. Geocarto Int, 35(7): 759–780
Lap B Q, Harada M, Hiramatsu K (2013). Dynamics of water quality in the Truc Bach Lake, Hanoi Capital, Vietnam. J Fac Agric Kyushu Univ, 58(1): 145–151
Lee Z, Shang S, Qi L, Yan J, Lin G (2016). A semi-analytical scheme to estimate Secchi-disk depth from Landsat-8 measurements. Remote Sens Environ, 177: 101–106
Lillesand T M, Johnson W L, Deuell R L, Lindstrom O M, Meisner D E (1983). Use of Landsat data to predict the trophic state of Minnesota lakes. Photogramm Eng Remote Sensing, 49: 219–229
Liu X, Meng X, Wang X, Bi D, Chen L, Lou Q (2020). Using a semi-analytical model to retrieve Secchi depth in coastal and estuarine waters. Acta Oceanol Sin, 39(8): 103–112
Matthews M W (2011). A current review of empirical procedures of remote sensing in inland and near-coastal transitional waters. Int J Remote Sens, 32(21): 6855–6899
Matthews M W, Bernard S (2013). Characterizing the absorption properties for remote sensing of three small optically-diverse South African reservoirs. Remote Sens, 5(9): 4370–4404
Membrillo-Abad A S, Torres-Vera M A, Alcocer J, Prol-Ledesma R M, Oseguera L A, Ruiz-Armenta J R (2016). Trophic State Index estimation from remote sensing of Lake Chapala, México. Rev Mex Cienc Geol, 33(2): 183–191
Mobley C D (1999). Estimation of the remote-sensing reflectance from above-surface measurements. Appl Opt, 38(36): 7442–7455
Mobley C D, Werdell J, Franz B, Ahmad Z, Bailey S (2016). Atmospheric correction for satellite ocean color radiometry. In: NASA Tech Memo, NASA/TM-2016–217551
Mouw C B, Greb S, Aurin D, DiGiacomo P M, Lee Z, Twardowski M, Binding C, Hu C, Ma R, Moore T, Moses W, Craig S E (2015). Aquatic color radiometry remote sensing of coastal and inland waters: challenges and recommendations for future satellite missions. Remote Sens Environ, 160: 15–30
Mueller J L, Morel A, Frouin R, Davis C, Arnone R, Carder K, Hooker S, Holben B, Mobley C D, McLean S, Miller M, Pietras C, Fargion G S, Knobelspiesse K D, Porter J, Voss K (2003). Ocean optics protocols for satellite ocean color sensor validation, Revision 4. In: Volume III: Radiometric Measurements and Data Analysis Protocols. Greenbelt
Nazeer M, Bilal M, Nichol J E, Wu W, Alsahli M M, Shahzad M I, Gayen B K (2020). First experiences with the Landsat-8 aquatic reflectance product: evaluation of the regional and ocean color algorithms in a coastal environment. Remote Sens, 12(12): 1938
Nguyen B T, Nguyen T B N, Duong T T, Le T M H, Pham Q L, Le D N, Le T P Q (2016). Preliminary investigations of organic pollution in water environment of some urban lakes in Hanoi city, Vietnam. J Vietnam Environ, 8(2): 107–113
Odermatt D, Gitelson A, Brando V E, Schaepman M (2012). Review of constituent retrieval in optically deep and complex waters from satellite imagery. Remote Sens Environ, 118: 116–126
Ogashawara I, Jechow A, Kiel C, Kohnert K, Berger S A, Wollrab S (2020). Performance of the Landsat 8 provisional aquatic reflectance product for inland waters. Remote Sens, 12(15): 2410
Olmanson L G, Brezonik P L, Finlay J C, Bauer M E (2016).

Comparison of Landsat 8 and Landsat 7 for regional measurements of CDOM and water clarity in lakes. Remote Sens Environ, 185: 119–128

Persson J (2012). Urban lakes and ponds. In: Bengtsson L, Herschy RW, Fairbridge R W, eds. Encyclopedia of Lakes and Reservoirs. Dordrecht, Netherlands: Encyclopedia of Earth Sciences Series. Berlin: Springer, 836–839

Pham Q V, Ha N T T, Pahlevan N, Oanh L T, Nguyen T B, Nguyen N T (2018). Using Landsat-8 images for quantifying suspended sediment concentration in Red River (northern Vietnam). Remote Sens, 10(11): 1841

Ren J, Zheng Z, Li Y, Lv G, Wang Q, Lyu H, Huang C, Liu G, Du C, Mu M, Lei S, Bi S (2018). Remote observation of water clarity patterns in Three Gorges Reservoir and Dongting Lake of China and their probable linkage to the Three Gorges Dam based on Landsat 8 imagery. Sci Total Environ, 625: 1554–1566

Rotta L, Alcântara E, Park E, Bernardo N, Watanabe F (2021). A single semi-analytical algorithm to retrieve chlorophyll-a concentration in oligo-to-hypereutrophic waters of a tropical reservoir cascade. Ecol Indic, 120: 106913

Schalles J F (2006). Optical remote sensing techniques to estimate phytoplankton chlorophylla concentrations in coastal. In: Richardson L L, LeDrew E F, eds. Remote Sensing of Aquatic Coastal Ecosystem Processes. Dordrecht: Springer, 22–79

Shi K, Zhang Y, Song K, Liu M, Zhou Y, Zhang Y, Li Y, Zhu G, Qin B (2019). A semi-analytical approach for remote sensing of trophic state in inland waters: Bio-optical mechanism and application. Remote Sens Environ, 232: 111349

Thủy, N B, Ngọc N T B, An V D, Quỳnh L T P, Nghĩa L D, Thủy D T, Cường H T (2017). Assessment of the trophic status in some lakes within Hanoi inner city. Vietnam J Sci Technol, 55(1): 84–92

USGS (2020a). Surface Reflectance Code (LASRC) Product Guide. Reston: USGS and NASA

USGS (2020b). Landsat Provisional Aquatic Reflectance Algorithm Description Document (ADD). Reston: USGS and NASA

Vermote E, Justice C, Claverie M, Franch B (2016). Preliminary analysis of the performance of the Landsat 8/OLI land surface reflectance product. Remote Sens Environ, 185(2): 46–56

Vietnam Institute of Meteorology, Hydrology and Climate Change (2019). Agricultural Meteorology Reports for June 2019. Available at Vietnam Institute of Meteorology, Hydrology and Climate Change website

Vietnamnet.vn (2016a). Waste and dead fish in Hanoi's lakes. Available at VietNamNet website

Vietnamnews.vn (2016). Văn Quán Lake polluted, stinking up locality: locals. Available at Vietnamnews website

Vietnamnews.vn (2018). Blue-green algae bloom in Hoàn Kiếm Lake. Available at Vietnamnews website

Vinh P Q, Ha N T T, Binh N T, Thang N N, Oanh L T, Thao N T P (2019). Developing algorithm for estimating chlorophyll-a concentration in the Thac Ba Reservoir surface water using Landsat 8 Imagery. Vietnam J Earth Sci, 41(1): 10–20

Vnexpress.net (2018). Toxic algae pose threat to Hanoi's iconic Sword Lake. Available at VnExpress website

Watanabe F S Y, Alcântara E, Rodrigues T W P, Imai N N, Barbosa C C F, Rotta L H D S (2015). Estimation of chlorophyll-a concentration and the trophic state of the Barra Bonita hydroelectric reservoir using OLI/Landsat-8 images. Int J Environ Res Public Health, 12(9): 10391–10417

Wunderground (2017). Historic heat wave sweeps Asia, the Middle East and Europe. Available at Wunderground website

Yang B, Ke X (2015). Analysis on urban lake change during rapid urbanization using a synergistic approach: a case study of Wuhan, China. Phys Chem Earth Parts ABC, 89: 127–135

Yang L, Ma K M, Zhao J Z, Bai X, Guo Q H (2007). The relationships of urbanization to surface water quality in four lakes of Hanyang, China. Int J Sustain Dev World Ecol, 14(3): 317–327

Zhou Y, He B, Xiao F, Feng Q, Kou J, Liu H (2019). Retrieving the lake trophic level index with Landsat-8 image by atmospheric parameter and RBF: a case study of lakes in Wuhan, China. Remote Sens, 11(4): 457

Zhu W, Huang L, Sun N, Chen J, Pang S (2020). Landsat 8-observed water quality and its coupled environmental factors for urban scenery lakes: a case study of West Lake. Water Environ Res, 92(2): 255–265

## AUTHOR BIOGRAPHIES

**Pham Quang Vinh** is an associate professor at Vietnam Academy of Science and Technology. He received his B.Sc. and Ph.D Degrees in Photogrammetry and Remote Sensing from Hanoi University of Mining and Geology (Vietnam) in 1983 and 2005, respectively. His current research interests include application of remote sensing for monitoring environmental changes and disaster impacts.

**Nguyen Thi Thu Ha** is an associate professor at VNU University of Science, Vietnam National University, Hanoi. She received her B.Sc and M.Sc Degrees in Geology from Vietnam National University, Hanoi (Vietnam) in 2000 and 2004, respectively and her Ph.D degree in Environmental and Life Science from Kumamoto University (Japan) in 2011. She is interested in monitoring water quality in coastal and inland waters using remote sensing date, and modeling vulnerability and resilience to geo-disasters.

**Nguyen Thien Phuong Thao** is a junior researcher at the Sea and Island Research Center of VNU University of Science, Vietnam National University, Hanoi. She received the B.Sc. and M.Sc. Degrees in Natural Resources and Environmental Management from VNU University of Science in 2016 and 2020, respectively. Her research interests include application of remote sensing for monitoring lake and river water quality and for mapping floods and drought disasters.

**Nguyen Thuy Linh** is a junior lecturer at VNU University of Science, Vietnam National University, Hanoi. She is currently pursuing the Ph.D Degree in Management of Resources and Environment at VNU University of Science (Vietnam). Her research focuses on assessing the impact of urbanization on water quality of lakes in Hanoi city (Vietnam).

**La Thi Oanh** received the B.Sc. Degree in Management of Resources and Environment from VNU University of Science, Vietnam National University, Hanoi (Vietnam). She has received the Master Degree at Department of Geomatics, Cheng Kung University (China) this year (2021). She is interested in developing AI models for image processing and estimating water constituents from Landsat and Sentinel 2 data.

**Luong Thi Phuong** is a junior researcher at The Alliance of Biodiversity International and CIAT, Hanoi, Vietnam. She received the B.Sc. and M.Sc. Degrees in Management of Resources and Environment at VNU University of Science (Vietnam). Her research interest includes analyzing, performing, and managing spatial data for environmental management.

**Nguyen Thi Thu Huyen** received the M.Sc. Degree in Cartography, Remote Sensing and GIS at VNU University of Science (Vietnam) in 2010. She is a researcher at Institute of Geography, Vietnam Academy of Science and Technology. Her research interest includes Cartography and GIS modeling.